# Collapse of thick-walled metal tubes with wide external grooves as controllable energy-dissipating devices

**S Salehghaffari**[1], **M Tajdari**[2*], and **F Mokhtarnezhad**[2]
[1]Department of Aerospace Engineering, Mississippi State University, Mississippi State, USA
[2]Department of Engineering and High Technology, Iran University of Industries and Mines, Tehran, Iran

*The manuscript was received on 7 May 2009 and was accepted after revision for publication on 16 June 2009.*

DOI: 10.1243/09544062JMES1709

**Q1** **Abstract:** This article focuses on the experimental and theoretical investigation of the axial crushing behaviour of thick-walled tubes with a number of wide grooves, cut from their outer surface, under both static and dynamic loading. While this structure is subjected to axial loading, plastic deformation occurs within the space of each wide groove, and thick portions (grooveless areas) control and stabilize the collapsing of grooved thick-walled tubes. Therefore, the kinetic energy is dissipated by the plastic collapsing of the structure between grooves. In the present study, quasi-static compression tests of specimens with various geometric parameters are performed. Dynamic tests of some specimens using a drop hammer apparatus are also carried out to study the dynamic effects on the collapsing and energy absorption behaviour of the shock absorber. Numerical simulations of axial crushing of the shock absorber under both quasi-static and impact loading, using LS-DYNA finite-element explicit code, are also carried out in this article, and their results are verified with experimental findings. Based on experimental studies, an analysis with consideration of strain hardening effects to predict mean crushing load and energy absorption of the structure under axial compression is developed. Through the performed experimental, numerical, and analytical studies, major parameters in the design of the shock absorber are characterized and possible collapse modes of deformation during axial crushing of the structure are identified. In the present study, experimental and theoretical studies show that the introduced structure can be considered as an efficient energy-dissipating device since it provides favourable crashworthiness characteristics.

**Keywords:** thick-walled tubes, thin-walled tubes, external grooves, energy absorbers, dynamic and quasi-static loading

## 1 INTRODUCTION

Energy-absorbing devices have been extensively used in all vehicles and moving parts such as road vehicles, railway couches, aircraft, ships, lifts, and machinery. The aim is to protect these structures from serious damage when subjected to impact load, or to minimize human injuries when collision occurrs in transportation systems. These energy-absorbing devices can dissipate kinetic energy in a wide variety of ways such as friction, fracture, plastic bending, crushing, cyclic plastic deformation, and metal cutting [**1**]. Also, various structures such as circular and square tubes, octagonal cross-section tubes, spherical shells, frusta, taper tubes, s-shaped tubes, composite tubes, honeycomb cells, and foam-filled and wood-filled tubes may be used as collapsible energy absorbers. Among them, metallic cylindrical tubes have attracted much more attention because of their high stiffness and strength combined with their low weight and ease of their manufacture, which leads to the low costs of energy-dissipating devices [**2**, **3**].

The use of thin-walled tubes to collapse plastically under axial compression has been considered as one of the most efficient means of energy absorption. Several theoretical and experimental investigations have been performed so far to introduce different methods of plastic collapse in these structures [**2**]. One

* *Corresponding author: Engineering and High Technology Department, Iran University of Industries and Mines, 12 KarimKhan Avenue, Tehran, Iran.*
**Q2** *email: tajdari@iuim.ac.ir*

of these energy-dissipating methods is to compress a tube against a rigid die, which may result in several different modes of deformation. Among them, the most favourable deformation mode from the point of energy absorption is the inversion mode, occurring within the specific range of geometrical dimensions for a tube and die along with a specific friction condition between them. Therefore, several researchers have performed both theoretical and experimental studies to improve the possibility of shaping a successful inversion mode while compressing a tube against rigid die [**4**–**7**]. Even though the inversion mode of deformation provides a favourable constant crush force, only a half of the tube length can contribute to plastic deformation and energy absorption. The axial splitting and curling of tubes against canonical dies is the other recognized method of energy dissipation, having been studied by a number of researchers [**7**–**10**]. In this energy-dissipating method, a great percentage of tube length contributes to the dissipation of external energy, and the collapsing force is relatively steady. However, this method provides low crush load and cannot be used in the protection of structures subjected to high impact loads.

To find different methods of encouraging thin-walled structures to collapse plastically, the axial crushing of cylindrical tubes has received considerably more attention. This method provides a reasonably constant load and fairly high crush force efficiency, and the greater percentage of tube material can contribute to plastic deformation while the structure crushes axially, providing a high specific energy absorption factor. However, all of these favourable crashworthiness characteristics can be achieved when the tube crushes in the concertina mode of deformation, and numerous numbers of experimental and theoretical studies [**11**–**18**] have shown that, depending on tube geometry, material properties of the tube, boundary conditions, and loading conditions, it may buckle in other modes of deformation such as diamond, Euler, and mixed modes. In fact, the Euler mode of deformation, occurring when the tube length is greater than the critical length for a given diameter and thickness of the tube, should be avoided in crashworthiness applications as this mode provides inefficient and unreliable crashworthiness characteristics of the energy absorber. On the other hand, although the diamond and mixed modes are considerably more likely to occur than other collapsing modes for a common dimension of the tube, little changes in the loading and boundary condition can easily cause a tube with the potential of crushing in the diamond or mixed modes to buckle in the Euler mode of deformation. In addition, even under fixed boundary and loading conditions, miscalculation is inevitable when the shock absorber is designed to collapse in the diamond or mixed mode of deformation since the exact shape of the tube in these cases is quite unpredictable. The concertina or axisymmetric collapsing mode has none of these limitations, and has been considered as the most reliable and efficient deformation mode in dissipating impact energy. Moreover, for a fixed length of the tube, the concertina mode takes more energy than the diamond mode because of the extra extensibility of the tube walls consumed by the concertina folds. Unfortunately, experimental studies show that among the wide range of tube dimensions, it can crush in concertina mode within the considerably limited region of the $L/D$ and $D/t$ diagram, over which the tube has less contribution in energy dissipation compared to larger ones.

As explained above, the efficiency of all these recognized methods in encouraging thin-walled tubes to collapse plastically and absorb energy strongly depends on the geometric and other specific design parameters of the shock absorber. This limits their application when engineers are faced with geometric limitation in the design of a collapsible shock absorber for a structure that may be subjected to shock loading. Moreover, the collapse of circular tubes in these limited geometric regions provides specific values of mean crushing load, which may not be the values required to protect some engineering structures. On the other hand, the efficiencies of these realized energy-absorbing methods are strongly sensitive to external parameters such as loading direction and conditions that limit their applications in the protection of some structures where collision may cause serious damage. In some structures, the shock absorber is considered to be one part of the structure that should also be capable of dissipating kinetic energy to protect other main parts from damage when the whole structure is subjected to shock loading. For these applications, a shock absorber with extreme deformation is not suitable. However, application of these methods in the collapse of cylindrical tubes leads to extreme plastic deformation of the energy-absorbing device, causing unfavourable instability of the structure while crushing.

However, so far there has been limited research to improve these deficiencies in the plastic collapse of thin-walled structures. In a recent research [**19**], cutting an initial circumferential edge groove outside the tube and using one- and two-circumferential stiffeners have been suggested as two design methods to activate the axisymmetric plastic buckling mode. In this research, several validated finite-element (FE) simulations have also shown the extension of the axisymmetric collapsing region after using these methods in the $L/D$ and $D/t$ diagrams. These two design methods reduce the maximum load due to the initial elastic resistance of a tube when subjected to axial impact load, improving the crush force efficiency of the shock absorber. In another research [**20**], cutting circumferential grooves alternatively inside and outside the tube at predetermined intervals have been introduced as a

solution to force the plastic deformation to occur at these predetermined intervals along the tube length. This proposed method could be a good candidate for a controllable energy absorption element, but it reduces the amount of material participating in plastic deformation and energy absorption. Cutting a given tubular structure in several portions and coaxially assembling them by separating the non-deformable disc is the other solution to encourage the axisymmetric mode in the axial crushing of tubes, investigated by Abdul-Latif *et al.* in reference [**21**]. The energy absorption characteristics of corrugated tubes are studied in reference [**22**]. In this energy-dissipating device, corrugations are introduced in the tube to force the plastic deformation to occur at predetermined intervals along the tube length. The aims are to improve the uniformity of the load–displacement behaviour of axially crushed tubes, and to predict and control the mode of collapse in each corrugation in order to optimize the energy absorption capacity of the tube. Investigations into the behaviour of tapered sheet metal tubes under axial and oblique dynamic loading have also been reported in references [**23**]and [**24**]. These studies show that tapered tubes can withstand oblique impact loads as effectively as axial loads. In the case of vehicular collisions, the height above the road, which is subjected to impact loads, remains reasonably constant but the direction of the acting force line is subjected to change in a horizontal plane. For such situations, tapered tubes of rectangular cross-section with a constant height but increasing width along its axial direction may prove to be advantageous. Recently, expansion of circular metal tubes by rigid tubes under axial compression has been introduced as an efficient method of dissipating energy without any strong sensitivity to loading uniformity [**25**]. Several attempts have also been made to improve the energy-absorbing capacity of metal tubes by using filler materials such as polymeric foams [**26–28**]. These researches have shown that filling cylindrical tubes with foams eliminates their non-compact crushing behaviour under axial loads and significantly helps in preventing global bending. Moreover, in comparison with empty tubes of the same size, foam-filled tubes are less affected by external parameters and are more stable while collapsing.

The objective of this investigation is to develop a design method to improve described deficiencies of different realized methods of encouraging plastic collapse in cylindrical tubes. In this innovative design method, circumferential wide grooves, which are cut from the outer surface of thick-walled cylindrical tubes, convert it into several thin-walled tubes of shorter length, being assembled together coaxially. Figure 1 shows the shape of a thick tube with wide external grooves as well as its detailed design. In fact, while this grooved structure is subjected to axial compression, plastic folds are shaped within each grooved space, and thick portions between grooved areas of

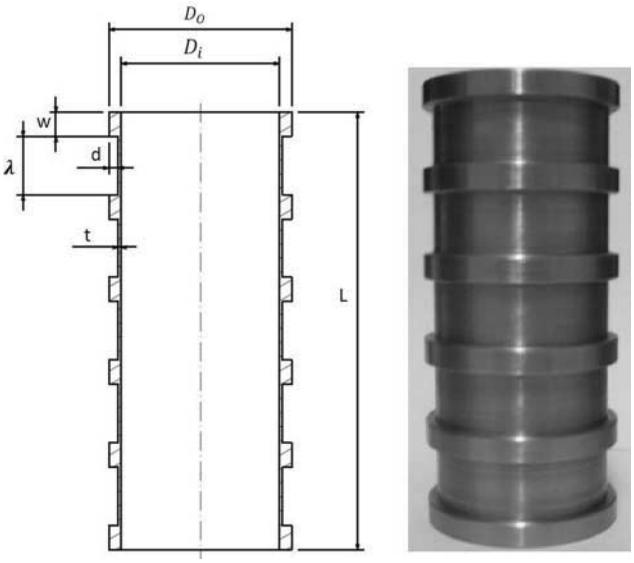


**Fig. 1** Shape of a tube with wide external grooves with its detailed design

the shock absorber control and stabilize the crushing process. In this design method, while grooveless thick areas of the shock absorber do not contribute to plastic deformation and energy absorption, they play a significant role in improving other crashworthiness characteristics like stability in axial crushing and safety factor. In this study, different axial quasi-static crushing tests as well as dynamic tests using a drop hammer apparatus on mild steel thick tubes with a number of wide external grooves are performed, and the resulting load–displacement curves are studied. To study the collapsing and energy absorption behaviour of the shock absorber in detail, the numerical simulation of a specimen's collapse under both dynamic and quasi-static loads using explicit FE LS-DYNA code is also carried out. In this study, theoretical formulations are developed to predict the energy absorption and mean crushing load of the shock absorber.

## 2 EXPERIMENTS: DESCRIPTION AND RESULTS

### 2.1 Quasi-static tests

Seamless mild steel tubes of commercial quality with 62 mm outside diameter and 48 mm inside diameter were machined to the required size and a length of 144 mm. Then, circumferential wide grooves of different lengths and depths were cut from the outer surface of tubes to prepare specimens for compression tests. Cut surface areas of all specimens were ground to improve their surface quality. Figure 1 shows the typical shape of the prepared specimen for the compression test, and Table 1 shows the geometric parameters of each prepared specimen. As is realized from this table, three geometric parameters, namely

**Table 1** Experimented specimen's dimensions

| Specimen no. | $L$ (mm) | $D_o$ (mm) | $D_i$ (mm) | $t$ (mm) | $d$ (mm) | $\lambda$ (mm) | $W$ (mm) | $N$ |
|---|---|---|---|---|---|---|---|---|
| A1[a] | 144 | 54 | 52 | 1 | – | – | – | – |
| S6 | 144 | 60 | 52 | 1 | 3 | 16.8 | 10 | 5 |
| S4 | 144 | 60 | 52 | 1 | 3 | 13.5 | 9 | 6 |
| S2 | 144 | 60 | 52 | 1 | 3 | 19.2 | 8 | 5 |
| A2[a] | 144 | 55 | 52 | 1.5 | – | – | – | – |
| S15 | 144 | 60 | 52 | 1.5 | 2.5 | 16.8 | 10 | 5 |
| S13 | 144 | 60 | 52 | 1.5 | 2.5 | 13.5 | 9 | 6 |
| S11 | 144 | 60 | 52 | 1.5 | 2.5 | 19.2 | 8 | 5 |

[a]Groove-less specimen.

depth, length, and number of grooves, vary from one specimen to another. Also, to show the extension of the axisymmetric collapsing mode in the axial crushing of tubes by using the proposed design method, two grooveless tubes of similar $L/D$ and $D/t$ with that of tubes with cut wide grooves were also made for compression tests.

In order to obtain the material data of the specimens, a quasi-static material test is performed on a strip, cut from them, using a standard tensile test machine and the resulting stress–strain relationship is shown in Fig. 2. The elastic modulus of this material is $E = 210$ GPa and its density is $\rho = 7800\,\text{kg/m}^3$. It is assumed that the mechanical properties of this steel alloy are not sensitive to strain rate at room temperature.

In this study, all quasi-static axial compression tests of specimens were performed on a 20 ton ZWICK hydraulic testing machine at a nominal crushing speed of 10 mm/min, and specimens were crushed between parallel steel plates of the test machine without any additional fixing. A repeated compression test of each specimen was also performed to ensure the validity of experimental results.

The final shapes of all specimens after the compression test are shown in Figs 3 and 4, and the corresponding load–displacement curves of two experimented

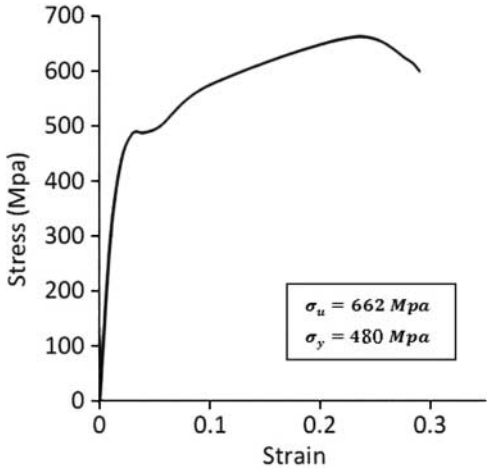


**Fig. 2** Stress–strain relationship of specimen's material

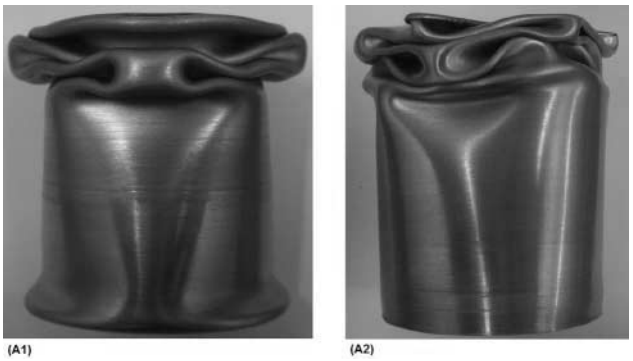


**Fig. 3** Groove-less specimens after quasi-static axial crushing

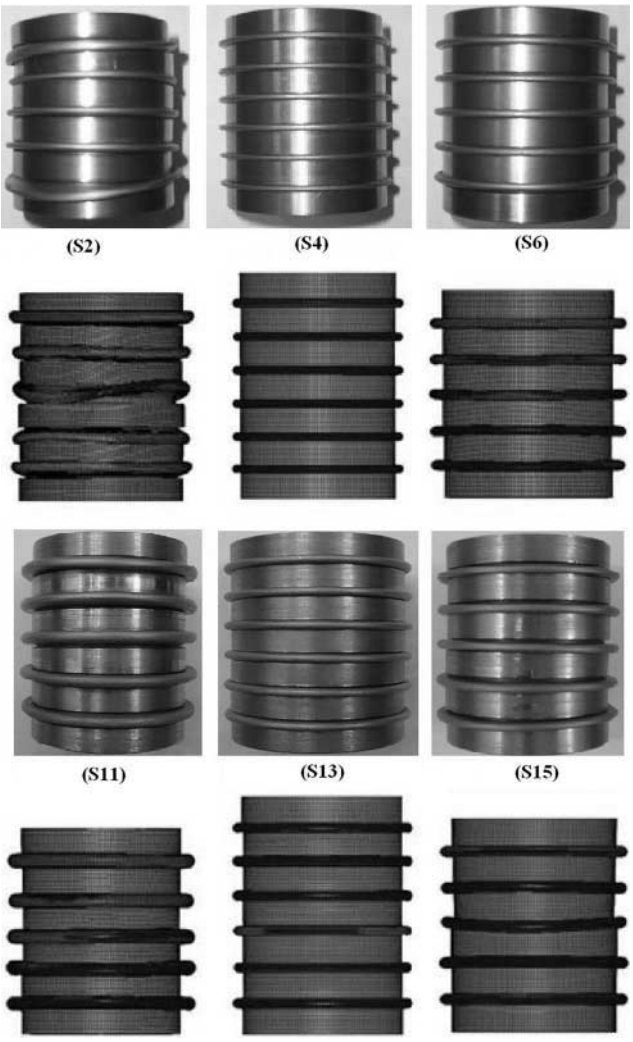


**Fig. 4** Grooved specimens after quasi-static axial crushing

specimens with concertina collapse mode are plotted in Fig. 5. Values of energy absorption and mean crushing loads were calculated by measuring the area under the obtained load–displacement curves, and a summary of test results is also shown in Table 2.

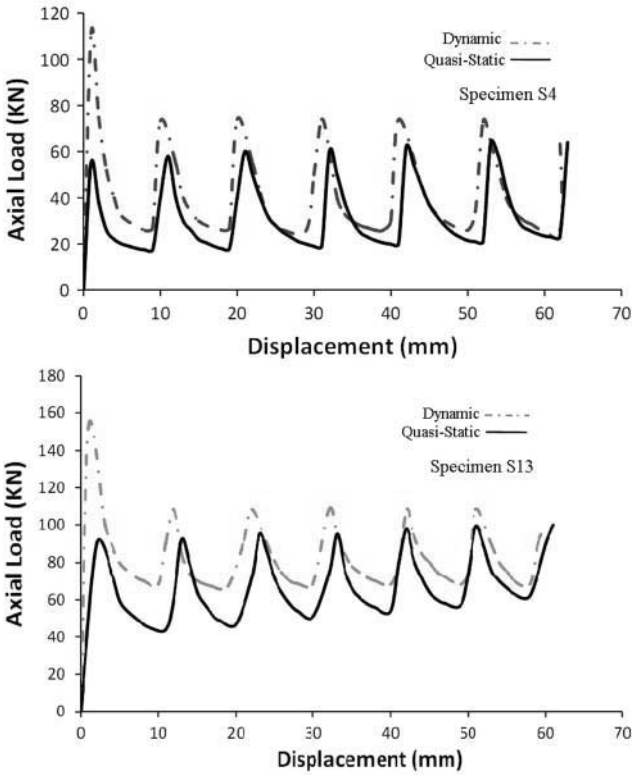


**Fig. 5** Dynamic and static load–displacement curves of specimens S4 and S13 during axial crushing derived from experimental tests

Comparison between the crushed shapes of grooveless tubes and of grooved ones shows the reliability of the proposed design method, developed in the present study, as it extends the limits of axisymmetric collapsing modes of deformation under axial compression significantly. In the present study, these experimental results are also used to verify theoretical studies of the proposed shock absorber.

## 2.2 Dynamic tests

In the present study, to compare the energy absorption characteristics of the shock absorber under dynamic loading with that under quasi-static loading, impact tests of specimens S4 and S13 with concertina collapsing mode under quasi-static compression are also performed. These impact tests were conducted on the drop hammer facility, shown in Fig. 6. As can be seen from this figure, in this drop hammer machine, both ends of the workpiece are fixed on an iron plate with a ditch. The mass of the drop weight in all conducted dynamic tests is constant and equal to 135 kg, but the height from which the weight can fall freely is adjustable. Therefore, the initial impact velocity of the 135 kg colliding mass depends on its falling position. The height of this colliding mass for the first impact test of specimen S13 was estimated from the quasi-static test data of this specimen to produce the kinetic energy of the falling mass around that absorbed in plastic deformation of the specimen under quasi-static compression. However, results show that this amount of colliding mass was not enough to shape concertina folds within all grooved areas of specimen

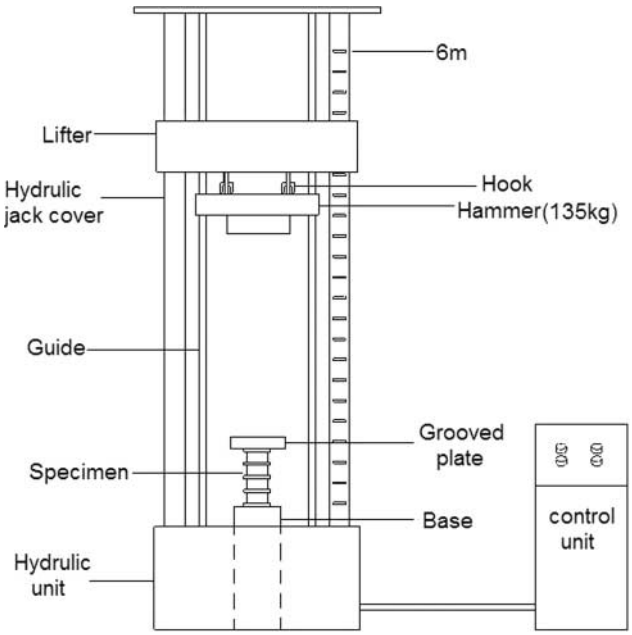


**Fig. 6** Drop hammer testing machine

**Table 2** Experimental, analytical, and numerical results of some specimens after quasi-static compression tests

| Specimen no. | Buckling mode[a] | $P_m$ (KN) | | | $E_T$ (J) | | |
|---|---|---|---|---|---|---|---|
| | | Test | FE | Analytic | Test | FE | Analytic |
| A1 | D | 26.52 | – | – | 1910.45 | – | – |
| S6 | 5C | 28.38 | 27.21 | 23.81 | 1759.56 | 1687.02 | 1762.25 |
| S4 | 6C | 29.23 | 29.15 | 23.79 | 1841.49 | 1836.45 | 1641.38 |
| S2 | 3C→D | 30.40 | 28.86 | 24.6 | 2280.00 | 2164.50 | 2115.45 |
| A2 | D | 44.06 | – | – | 2820.17 | – | – |
| S15 | 5C | 53.03 | 52.79 | 46.83 | 3287.86 | 3272.98 | 3231.58 |
| S13 | 6C | 57.36 | 57.29 | 50.08 | 3441.60 | 3437.40 | 3154.98 |
| S11 | 5C | 50.32 | 50.19 | 46.53 | 3673.36 | 3663.87 | 3769.21 |

[a]C, concertina and D, diamond.

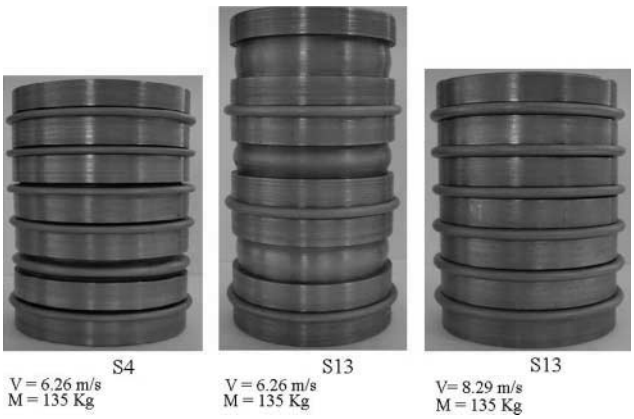


**Fig. 7** Crushed shape of specimens S4 and S13 after impact tests

**Table 3** Experimental and numerical results for specimens S4 and S13 after impact tests

| Specimen no. | Buckling mode[a] | $M$ (kg) | $V$ (m/s) | $P_m$ (KN) Test | $P_m$ (KN) FE | $E_T$ (J) Test | $E_T$ (J) FE |
|---|---|---|---|---|---|---|---|
| S4 | 6C | 135 | 6.26 | 42.03 | 40.87 | 2648.73 | 2610.63 |
| S13 | 6C | 135 | 8.29 | 77.67 | 75.94 | 4661.71 | 4557.88 |

[a]C, concertina.

S13 (see Fig. 7). This is because material strain rate sensitivity increases the energy absorption capacity of the shock absorber under impact loading. Therefore, a strain rate sensitivity factor of around 1.4 was used in calculating the appropriate height of the colliding mass since it was anticipated that an increase in energy dissipation of 1.4 times the quasi-static levels would be achieved under impact loading conditions for the second test of specimen S13 and the first test of specimen S4. The condition of the impact test for each experimented specimen as well as their test results are shown in Table 3. The final shapes of all specimens after the impact test are shown in Fig. 7, and their corresponding load–displacement curves are plotted in Fig. 5.

## 3 ANALYTICAL MODEL

The axisymmetric collapse shape of the shock absorber under axial compression (see Fig. 4) shows that one concertina fold is shaped within the space of each wide groove over axial compression of the structure. According to this observation, a simple collapse model of the shock absorber is shown in Fig. 8. This collapse model shows that during the formation of one axisymmetric convolution within one grooved space, three circumferential plastic hinges occur within the space of one external wide groove and the metal between its surface experiences stretching. Therefore, the required plastic energy in the formation of

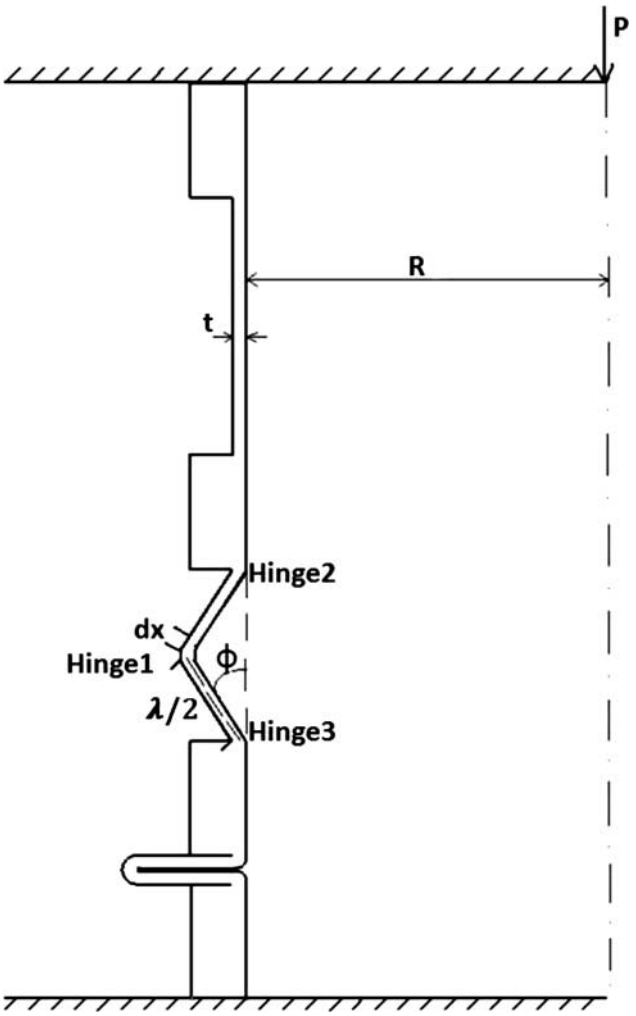


**Fig. 8** Collapse model of externally grooved thick-walled tube

one axisymmetric fold ($E_D$) is the sum of the energy absorbed in the formation of three assumed stationary circumferential plastic hinges ($E_b$) and the energy absorbed in expansion because of high circumferential stresses between these hinges ($E_s$). Hence, we have the following expression for the total required plastic energy in the formation of one axisymmetric fold between each grooved space

$$E_D = E_b + E_s \tag{1}$$

To analyse equation (1), the following assumptions are made in the present study.

1. The elastic strain is neglected.
2. The strain hardening in plastic hinges is neglected.
3. The material flow curve of the shock absorber obeys the equation $\bar{\sigma} = k\bar{\varepsilon}^n$.
4. Change in wall thickness at any point of the grooved tube is small.
5. Circumferential hinges in axisymmetric buckling are considered to be stationary.

6. Angle $\phi$ increases from zero to a value of $\sim\pi/2$. Therefore, the buckling process in the formation of one convolution within a groove space of the shock absorber is complete when the straight-sided convolutions come in contact.

From Alexander's theory [**29**], the energy absorbed in three stationary plastic hinges (hinges 2, 3, and 1 in Fig. 8) is given as

$$W_b = 2M_P \int_0^{\pi/2} \left[ 2\pi R \, d\phi + 2\pi \left( R + \frac{\lambda}{2} \sin\phi \right) d\phi \right] = 2\pi M_P (2R\pi + \lambda) \quad (2)$$

where the plastic bending moment per unit circumferential length of the hinge using the von Mises criterion is $M_P = (2/\sqrt{3})\sigma_y(t^2/4)$.

The required energy for stretching the metal between each groove space in the formation of one axisymmetric plastic fold is

$$dE_s = \sigma_h \varepsilon_h \, dV \quad (3)$$

where the hoop strain $\varepsilon_h$ is given as

$$\varepsilon_h = \mathrm{Ln}\left( \frac{R + x\sin\phi}{R} \right) \approx \frac{x}{R} \quad (4)$$

The hoop stress is expressed in terms of effective stress, based on the stress condition between plastic hinges, as

$$\sigma_h = \frac{2}{\sqrt{3}} \bar{\sigma} \quad (5)$$

The hoop strain is expressed in terms of effective strain, based on the strain condition between plastic hinges, as

$$\varepsilon_h = \frac{\sqrt{3}}{2} \bar{\varepsilon} \quad (6)$$

Substituting equations (5) and (6) into the flow curve equation, we have

$$\sigma_h = \left( \frac{2}{\sqrt{3}} \right) k \left( \frac{2}{\sqrt{3}} \varepsilon_h \right)^n = \left( \frac{2}{\sqrt{3}} \right)^{n+1} k \left( \frac{x}{R} \right)^n \quad (7)$$

Substituting equations (7) and (4) into equation (3), we have the following expression for the energy absorbed in expansion because of high circumferential stresses between the hinges in the formation of one axisymmetric plastic fold

$$E_s = (4\pi R t k) \left( \frac{2}{\sqrt{3}} \right)^{n+1} \int_0^{\lambda/2} \left( \frac{x}{R} \right)^{n+1} dx = \frac{2k\pi t \lambda^{n+2}}{(n+2)(\sqrt{3})^{n+1} R^n} \quad (8)$$

Substituting equations (8) and (2) into equation (1), we have the following expression for the total required plastic energy in the formation of one axisymmetric fold between each grooved space

$$E_D = \left( \frac{\pi t^2 \sigma_y}{\sqrt{3}} \right) (2R\pi + \lambda) + \frac{2k\pi t \lambda^{n+2}}{(n+2)(\sqrt{3})^{n+1} R^n} \quad (9)$$

### 3.1 Total absorbed energy in plastic deformation

Multiplying equation (9) by the number of grooved spaces of the shock absorber $N$, we have the following equation for the total amount of energy absorbed by the shock absorber in plastic collapse after the compression test is complete

$$E_T = N\pi t \left[ \left( \frac{t\sigma_y}{\sqrt{3}} \right) (2R\pi + \lambda) + \frac{2k\lambda^{n+2}}{(n+2)(\sqrt{3})^{n+1} R^n} \right] \quad (10)$$

### 3.2 Total absorbed energy of the shock absorber per weight

The total weight of the presented shock absorber will be (see Fig. 1)

$$G = \rho\pi \left[ N\lambda D_i t + (N+1) W \frac{(D_i^2 - D_o^2)}{4} \right] \quad (11)$$

Therefore, the total absorbed energy per weight for the presented shock absorber will be

$$S_e = \frac{E_T}{G} = \frac{Nt\{(t\sigma_y/\sqrt{3})(2R\pi + \lambda) + [2k\lambda^{n+2}/(n+2)(\sqrt{3})^{n+1} R^n]\}}{\rho\{N\lambda D_i t + (N+1) W [(D_i^2 - D_o^2)/4]\}} \quad (12)$$

### 3.3 Mean crushing load

According to Fig. 1, the external work done in the formation of one axisymmetric fold within each grooved space is

$$W_T = P_m \times (\lambda - 2t) \quad (13)$$

Since the external work in the formation of one plastic fold is dissipated by the total energy absorbed in plastic formation of one convolution, the energy balance equation will be

$$W_T = E_D \quad (14)$$

Substituting equations (13) and (9) into equation (14), the mean crushing load of the shock absorber will be

$$P_m = \left[ \frac{\pi t}{(\lambda - 2t)} \right] \left[ \left( \frac{t\sigma_y}{\sqrt{3}} \right) (2R\pi + \lambda) + \frac{2k\lambda^{n+2}}{(n+2)(\sqrt{3})^{n+1} R^n} \right] \quad (15)$$

## 4 FINITE-ELEMENT SIMULATION OF QUASI-STATIC AND IMPACT TESTS

In the present study, numerical simulations of the axial crushing of 18 specimens under quasi-static compression were carried out using explicit FE code LS-DYNA, version 971. Geometric parameters of these numerically simulated specimens are shown in Table 4. To perform these numerical simulations, the basic three-dimensional (3D) geometry of the model was first created according to the user code [**30**]. In this 3D model, a rigid plate is placed on both the top and the bottom of the tube with wide external grooves. The bottom rigid plate is constrained in all degrees of freedom while the top plate was described as a rigid body with five constraints, assuming that only displacement along the vertical axis is allowed with a constant velocity. Thus, under this loading condition, no inertial effects on the forming mechanism are likely to occur and no dynamics effects in deformation mechanics need to be taken into account. Unlikely, in case of simulating the impact tests of specimens S4 and S13, this rigid top plate with a mass of 135 kg collides with the top end at initial velocities of 6.26 and 8.29 m/s, respectively.

To define contact between the movable rigid plate and the tube as well as between the tube and the fixed plate, 'surface-to-surface' contact type is used. In this 'surface-to-surface' contact description, tube nodes are defined as 'slave' nodes, whereas rigid plate nodes are 'master' nodes. A 'single-surface' interface is also selected to simulate the collapse of specimens when elements of the tube wall contact each other, creating a new interface. This contact type uses nodal normal projections; hence, it prevents elements from penetrating the specimen surface during collapse.

**Table 4** Geometric parameters of numerically simulated specimens subjected to quasi-static test

| Specimen no. | $L$ (mm) | $D_o$ (mm) | $D_i$ (mm) | $t$ (mm) | $d$ (mm) | $\lambda$ (mm) | $W$ (mm) | $N$ |
|---|---|---|---|---|---|---|---|---|
| S1 | 144 | 60 | 52 | 1 | 3 | 9 | 8 | 8 |
| S2 | 144 | 60 | 52 | 1 | 3 | 19.2 | 8 | 5 |
| S3 | 144 | 60 | 52 | 1 | 3 | 26 | 8 | 4 |
| S4 | 144 | 60 | 52 | 1 | 3 | 13.5 | 9 | 6 |
| S5 | 144 | 60 | 52 | 1 | 3 | 18 | 9 | 5 |
| S6 | 144 | 60 | 52 | 1 | 3 | 16.8 | 10 | 5 |
| S7 | 144 | 60 | 52 | 1 | 3 | 23.5 | 10 | 4 |
| S8 | 144 | 60 | 52 | 1 | 3 | 14.4 | 12 | 5 |
| S9 | 144 | 60 | 52 | 1 | 3 | 21 | 12 | 4 |
| S10 | 144 | 60 | 52 | 1.5 | 2.5 | 9 | 8 | 8 |
| S11 | 144 | 60 | 52 | 1.5 | 2.5 | 19.2 | 8 | 5 |
| S12 | 144 | 60 | 52 | 1.5 | 2.5 | 26 | 8 | 4 |
| S13 | 144 | 60 | 52 | 1.5 | 2.5 | 13.5 | 9 | 6 |
| S14 | 144 | 60 | 52 | 1.5 | 2.5 | 18 | 9 | 5 |
| S15 | 144 | 60 | 52 | 1.5 | 2.5 | 16.8 | 10 | 5 |
| S16 | 144 | 60 | 52 | 1.5 | 2.5 | 23.5 | 10 | 4 |
| S17 | 144 | 60 | 52 | 1.5 | 2.5 | 14.4 | 12 | 5 |
| S18 | 144 | 60 | 52 | 1.5 | 2.5 | 21 | 12 | 4 |

Solid elements (hex8) are used to model all the analysed tubes with wide external grooves. After convergence, an element size of 1 mm is found to produce suitable results. The material properties of the deformable tube are defined as elastic–plastic with kinematic hardening (material model type 3). Both fixed and movable plates are simulated using the 'material model type 20'. To remove hourglass mode, 'control-hourglass' is used, and for hourglass viscosity type (IHQ), equation (6) is considered as a suitable option.

## 5 VERIFICATION OF ANALYTICAL AND THEORETICAL MODELS

The experimental, analytical, and numerical values of mean crushing load and energy absorption of six specimens with different geometric parameters under quasi-static compression are compared in Table 2. These comparisons indicate that both analytical and numerical models, developed in this study, can predict mean crushing load and energy absorption of the axial collapse of externally grooved thick-walled cylindrical tubes under the quasi-static loading condition with great accuracy. It should be noted that in analytical calculations of the mean crushing load and energy absorption of these six specimens, strain hardening factors of $k = 550$ MPa and $n = 0.25$ (values recommended for mild steel) are employed, and the yield stress of the material is assumed to be $\sigma_y = 480$ MPa. Collapsed shapes of 18 specimens after quasi-static compression, which resulted from numerical simulations, are shown in Fig. 9. A comparison of some of these simulated collapsed shapes with corresponding experimented collapsed shapes shows that the presented FE model can simulate the crushed shape of the shock absorber after quasi-static compression with sufficient accuracy (see Fig. 4). Simulated crushing results of specimens S4 and S13 under impact loading are also compared with their experimental results. Comparisons indicate that there is good agreement between experimental results and those of performed FE analysis for crushing simulation of the shock absorber under dynamic loading (see Table 3 as well as Figs 7 and 10).

## 6 GEOMETRIC EFFECTS ON COLLAPSE MODE AND ENERGY ABSORPTION CHARACTERISTICS OF THE SHOCK ABSORBER

Various experimental tests and numerical simulations of specimens with different values of groove depth and length while crushing axially have shown that these geometric parameters can significantly affect the collapse modes of externally grooved thick-walled cylindrical tubes. Among these different collapse modes

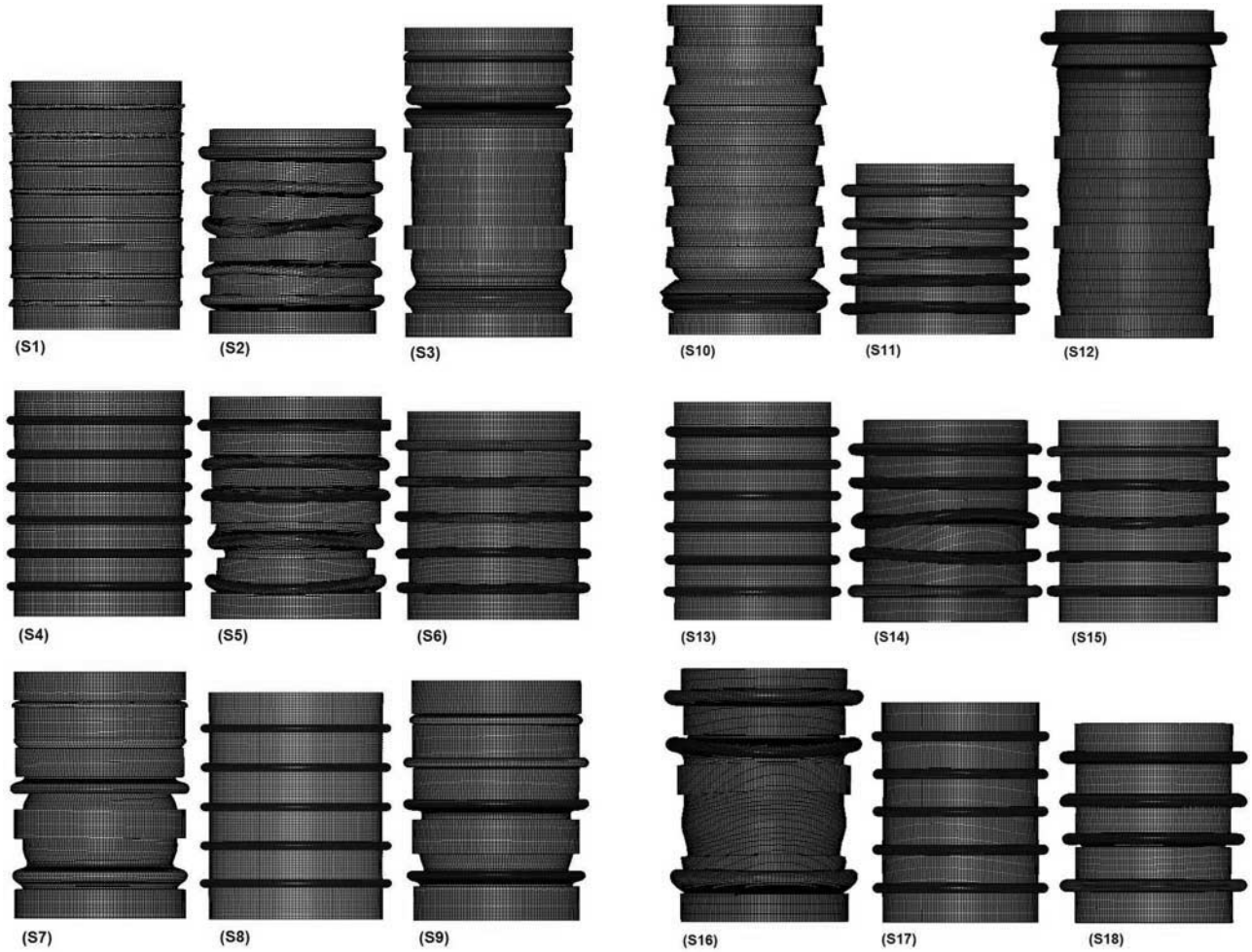


**Fig. 9** Crushed shapes of grooved specimens after quasi-static test derived from numerical simulation

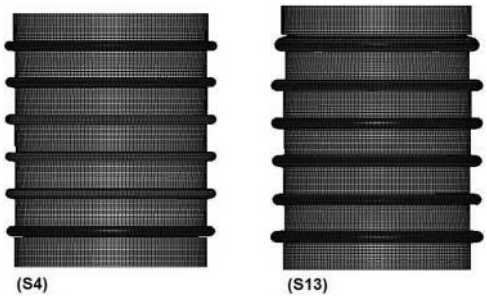


**Fig. 10** Crushed shapes of specimens S4 and S13 after impact test derived from numerical simulation

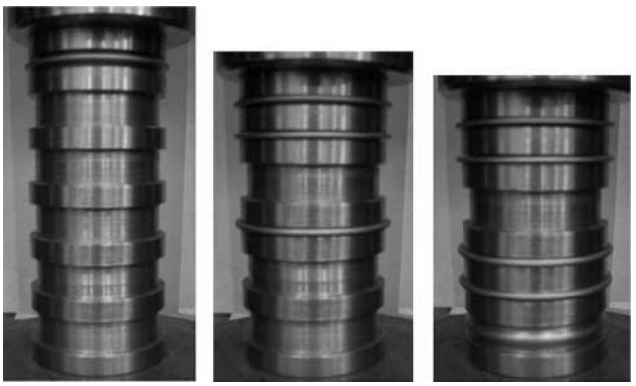

**Fig. 11** Views of different stages of axisymmetric buckling in specimen S4, derived from experimental tests

of deformation occurring within different values of groove depth and length for a given geometry of a thick-walled tube, the axisymmetric crushing mode of deformation provides the most favourable crashworthiness characteristics of the structure from the viewpoint of energy dissipation. Views of different stages of axisymmetric buckling in specimens S4 and S13 are shown in Figs 11 and 12. These figures show that collapse of the present shock absorber in axisymmetric mode is quite stable since thick areas of the structure (grooveless portions) move only in the axial direction without any deformation. Also, it can be seen that this collapse mode takes more energy because of the extra extensibility of the tube walls between thick portions compared to other possible modes, which will be studied in the present study later.

**Fig. 12** Views of different stages of axisymmetric buckling in specimen S13, derived from experimental tests

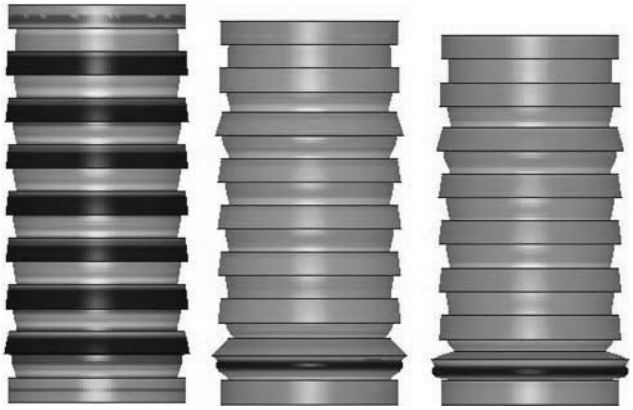

**Fig. 13** Views of different stages of axial crushing in specimen S10, derived from numerical simulation

Different stages of axisymmetric buckling in specimens S4 and S13 (see Figs 11 and 12) indicate that the creation of two stationary plastic hinges in the top and bottom areas of each groove's space along with the creation of the other plastic hinge in the middle of each groove space are necessary in the formation of one axisymmetric convolution within one groove space. In fact, while two plastic hinges in the top and bottom areas of each groove space in specimens S4 and S13 with axisymmetric collapse mode are stationary when subjected to axial compression, the third plastic hinge, forming in the middle space of these two stationary hinges, moves towards the outside of the structure till one straight-sided convolution, formed between the top and middle hinges, comes in contact with the other one, formed between the middle and bottom hinges, in one grooved space. Therefore, for a given geometry of a thick-walled cylindrical tube, the length and depth values of wide grooves, cut from its outer surface, should be arranged in such a way that the similar mechanism of plastic deformation, being described above in relation with axisymmetric collapse of specimens S4 and S13, occurs within each grooved space to guarantee axisymmetric collapse and favourable energy absorption characteristics of the structure while subjecting to axial compression.

As will be explained in detail soon, in specimens with shorter groove length of the critical length for the formation of an axisymmetric fold between them, two plastic hinges are shaped instead of three, being essential for the formation of one axisymmetric fold. In these specimens, elimination of the middle plastic hinge because of the considerable shortness of the groove's length results in the formation of wrinkles instead of an axisymmetric fold. Therefore, the described unfavourable mechanism of deformation occurs in the collapse of these specimens instead of the favourable ones, occurring in the concertina collapse mode of the shock absorber. This unfavourable mechanism of deformation, leading to the formation of wrinkles between each grooved space, occurs in the axial crushing of specimen S10 with 9 mm groove length and 2.5 mm groove depth. Figure 13 depicts different stages of plastic deformation and axial crushing of this specimen. As can be seen from this figure, in specimen S10, during the formation of plastic wrinkles within a groove space, one end of the thick area in connection with this grooved space is stretched towards inside of the tube and the other end of this thick area is stretched towards outside of it, deforming this cylindrical thick area before axial compression to a truncated cone after compression. This phenomenon completely destroys the crushing stability of the structure. As a matter of fact, plastic deformation within a grooved space in specimen S10 competes with the deformation of a connected grooveless thick area to this grooved space, leading to its radial deformation and hoop stretching. However, in specimen S1 with a grooved area 0.5 mm thinner than that in specimen S10, a 9 mm groove length is enough for collapsing the structure in concertina mode (see Fig. 14). In fact, grooved areas in specimen S1 are significantly weaker than thick areas of the shock absorber structurally, and deform before deformation of the thick portions starts. Therefore, unlike specimen S10, crushing of specimen S1 is quite stable since thick portions in this specimen move in the axial direction without any deformation. It is worth noting that, like Euler buckling mode in ordinary grooveless cylindrical tubes, the recognized mode of deformation in specimen S10 should be strongly avoided in the design of grooved thick-walled cylindrical tubes as energy-dissipating devices since axial crushing of the device in this mode is quite unstable, providing unfavourable crashworthiness characteristics.

Experimental and numerical studies also show that in specimens with a longer groove's length of the critical length for the formation of concertina fold within them, two different modes of deformation, namely twisted concertina and mixed (concertina and wrinkles) modes, occur over their axial crushing. As

**Fig. 14** Views of different stages of axial crushing in specimen S1, derived from numerical simulation

can be realized from Fig. 9, among specimens with a groove depth of 3 mm, specimens S2 and S5 and, among those with a groove depth of 3 mm, specimen S16 collapse in a twisted concertina mode of deformation. Hence, for specimens with a groove depth of 3 mm, the critical length over which the concertina mode cannot occur is 16.8 and this critical length for those specimens with a groove depth of 2.5 mm is 21 mm. This indicates that for a given geometry of a tube, critical values of groove lengths for the formation of concertina folds vary with values of groove depth. Figure 15 shows different stages of twisted concertina collapse mode in specimen S2. From this figure it can be realized that in this collapse mode, two plastic hinges are formed near the two ends of a groove's space and the third hinge is formed in the mid distance between them. At first, one axisymmetric fold is shaped with these three hinges, but further compression of the shock absorber results in stretching and bending of the material between this shaped axisymmetric fold and two ends of the groove's space. This phenomenon twists the shaped concertina fold, and creates the twisted concertina collapse mode of the structure. Like the axisymmetric mode of deformation, crushing of the shock absorber in twisted concertina collapse mode is still stable. However, this collapse mode provides slightly less specific energy absorption compared to that in the concertina collapse mode.

From Fig. 9, it is obvious that while the grooved length of the shock absorber becomes considerably longer than the critical length for the formation of concertina folds, the mixed collapse mode, which is the combination of concertina fold with diamond fold or wrinkles, occurs instead of the twisted concertina mode. This mode of deformation occurs in specimens S3, S7, S9, and S12 (see Fig. 9). Different stages of plastic deformation in specimens S3, S7, and S12 during their axial crushing are shown in Figs 16, 17, and 18, respectively. As can be seen from these figures, in mixed collapse mode, at the first stages of deformation, two plastic hinges are shaped near one end of the groove's space and the third hinge is

**Fig. 16** Views of different stages of axial crushing in specimen S3, derived from numerical simulation

**Fig. 15** Views of different stages of axial crushing in specimen S2, derived from numerical simulation

**Fig. 17** Views of different stages of axial crushing in specimen S7, derived from numerical simulation

**Fig. 18** Views of different stages of axial crushing in specimen S12, derived from numerical simulation

formed between their mid distances. After the formation of a plastic fold through these three hinges, further compression results in stretching and bending of the material between this shaped fold and the other end of the groove's space. This phenomenon leads to the formation of another diamond fold in specimen S3 (see Fig. 16) or wrinkles and a diamond fold in specimens S7 and S12 (see Figs 17 and 18) near the other end of the groove's space. It is obvious that collapse of the shock absorber in mixed mode of deformation provides a less specific energy absorption factor compared to that in the twisted concertina collapse mode. This is because the amount of material participating in the formation of the diamond fold and wrinkles in the mixed mode is bigger than that in the twisted concertina one. As can be seen from Figs 16 to 18, collapse of the shock absorber in the mixed collapse mode is still stable. However, the deformation of thick areas (grooveless portions) is obvious in specimen S12. In fact, grooved areas in this specimen are thick (1.5 mm) and long (26 mm) and this strengthen them structurally, leading to deformation of the thick portion over their plastic forming. Deformation of the thick portions in specimen S3 with a similar value of groove length to specimen S12 but with less thickness of the grooved areas (1 mm) is not obvious since in this specimen, unlike specimen S12, these grooved areas are structurally weaker than the thick portions.

From the collapse mechanism of the externally grooved thick-walled tubes, it can be realized that thick portions do not have any contribution in energy absorption during their axial crushing. However, these parts provide significant advantages, which in some special engineering applications outweigh the disadvantage of getting the presented energy-absorbing device heavy. They play a significant role in improving the stability of the shock absorber while crushing. In some engineering structures, the shock absorber is considered as one part of the structure that should also be capable of dissipating kinetic energy to protect the other main parts from damage when the structure is subjected to shock loading. For these applications, a shock absorber with extreme deformation is not suitable. Thick portions in the proposed energy-dissipating device meet these demands and prevent extreme plastic deformation of the shock absorber, causing unfavourable instability, while crushing. Another advantage is that these portions make a significant contribution to encourage the shock absorber to collapse in the concertina mode, leading to a significant increase in the safety factor.

As was explained earlier, the deformation of thick portions in some specimens (S10, S12, and S16) over their axial compression reduces their crushing stability. One solution to avoid this phenomenon is to make the grooveless areas of the shock absorber structurally stronger by lengthening these thick parts. Another solution is to make the grooved areas of the shock absorber structurally weaker by decreasing their thickness or length. The deformation of thick portions in specimens with grooved areas of 1 mm thickness is considerably less significant than in specimens with grooved areas of 1.5 mm thickness, and this verifies the validity of the mentioned solution. However, these solutions of improving the stability of the shock absorber crushing lead to reduction of its specific energy absorption factor. In fact, geometric parameters of the shock absorber should be arranged in a way that provides the optimum specific energy absorption factor while maintaining its crushing stability.

Numerical and experimental studies also indicate that in specimens with large groove lengths, decreasing the depth of the groove, cut from their outer surface, can control the buckling mode of deformation. In fact, for specimens with a groove depth of 3 mm, the critical length over which the concertina mode cannot occur is 16.8, and this value is increased to 21 mm by decreasing the groove's depth of specimens to 2.5 mm. Table 2 also indicates that values of both the length and the depth of grooves, cut from the outer surface of the tube, can affect the mean crushing load of the shock absorber; however, the effect of groove depth is considerably more significant. Therefore, mean crushing load and buckling mode of deformation in the discussed energy absorber of this study can be controlled by the geometry of the tube and both values of groove depth and length, cut from its outer surface.

## 7 LOAD–DISPLACEMENT CURVES

### 7.1 Quasi-static loading

Figures 11 and 12 show different stages of axisymmetric buckling in specimens S4 and S13 when subjected to quasi-static compression. As is realized from these figures, at the first stage of buckling, one fold tends to

shape within the length of the nearest groove to the bottom end of the specimen when the shock absorber is compressed quasi-statically. During this stage of deformation, the load increases because of the elastic resistance of the divided structure along this groove length, and declines dramatically when a plastic fold shapes completely within this groove space (see Fig. 5). At the next stage of buckling, the second fold tends to shape within the length of another groove, near the former shaped groove with the concertina fold. At this stage of deformation, again, the load increases as a result of elastic resistance of the divided structure along this groove length, and declines dramatically when a plastic fold shapes completely within this groove space (see Fig. 5). As compression of the shock absorber continues, the same phenomenon tends to occur within the space of other wide grooves, leading to a sharp increase and decrease of load, till the buckling process of the shock absorber becomes complete (see Figs 5 and 11).

### 7.2 Dynamic loading

Different stages of axisymmetric buckling in specimens S4 and S13, resulting from numerical simulations, under dynamic loading are shown in Figs 19 and 20. A comparison of the corresponding load–displacement curves for these specimens under dynamic loading with those under quasi-static loading, resulting from experimental tests, is also shown in Fig. 5. This figure shows that the dynamic force at the initial stage of deformation for both specimens is considerably higher than the quasi-static load. In fact, this observed difference has to be associated with inertia effects set up at the instant of impact because of the lateral movements of sidewalls within all grooved spaces of the whole structure in order to initiate the folding process between them. Also, the strain rate effects of material within each grooved space should not be neglected in this observed difference between related dynamic and quasi-static forces to the initial stage of deformation, although these effects are less significant compared with inertia effects. However, as can be seen from Fig. 5, except for the considerable fluctuation of dynamic load at the initial deformation stage, these fluctuations in the formation of later concertina folds within grooved spaces over the rest of the time are significantly less than those of quasi-static load in the formation of concertina folds. In case of dynamic loading, inertia effects set up at the instant of impact cause lateral movements of the sidewalls within all grooved spaces of the whole structure and initiate the folding process between them. This phenomenon significantly reduces the elastic resistance of the divided structure within each grooved space during the rest of the time over which the whole structure is subjected to dynamic loading. However, in case of quasi-static compression, prior to the formation of one concertina fold between one grooved space, the load should overcome the elastic resistance of the divided structure at any stage of plastic deformation. The ratio of both dynamic and quasi-static minimum loads to maximum load in the formation of one concertina fold for specimens S4 and S13 is shown in Table 5. The mean crushing load and energy absorption capacity of the shock absorber under dynamic loading are considerably more than under quasi-static compression because of the material strain rate sensitivity effects and less fluctuation of dynamic loading in the formation of concertina folds between grooved spaces (see Table 3). However, the dynamic crush force efficiency of the shock absorber is slightly less than the quasi-static one.

Figure 20 indicates that unlike the sequence of plastic deformation within grooved areas of specimen S13 under quasi-static compression, in case of dynamic loading, shaping of the concertina folds starts from the grooved space nearest the top end of this specimen. As for specimen S4, under dynamic loading like quasi-static loading, the first concertina fold is shaped

**Fig. 19** Views of different stages of axisymmetric buckling in specimen S4 under dynamic loading, derived from numerical simulation

**Fig. 20** Views of different stages of axisymmetric buckling in specimen S13 under dynamic loading, derived from numerical simulation

**Table 5** Comparison between applied dynamic and quasi-static loading parameters of the shock absorber

| Specimen no. | $\frac{P_{\text{mDynamic}}}{P_{\text{mStatic}}}$ | $P_{\max}$ (KN) | | $\frac{P_{\min\text{ fold}}}{P_{\max\text{ fold}}}$ | |
|---|---|---|---|---|---|
| | | Quasi-static | Dynamic | Quasi-static | Dynamic |
| S4 | 1.438 | 61.11 | 111.22 | 0.292 | 0.353 |
| S13 | 1.354 | 94.39 | 152.91 | 0.525 | 0.626 |

within the length of the nearest groove to the bottom end of this specimen. However, the later concertina fold is shaped within the grooved space in the middle of the shock absorber length for the dynamic loading condition. The shaping sequence of other concertina folds of this specimen under dynamic loading, being different with that under quasi-static loading, can be seen from Fig. 19.

## 8 ENERGY ABSORPTION CHARACTERISTICS OF THE SHOCK ABSORBER

In the present study, to show the efficiency of the proposed method in extending the limits of the axisymmetric mode of deformation, for each set of grooved specimens with fixed groove depth, a grooveless specimen of the same geometric parameters has been compressed axially. Corresponding results show that (see Figs 3 and 4) introduction of wide grooves on the outer surface of cylindrical tubes can control the axisymmetric collapsing mode of the shock absorber considerably. Comparison between different stages of axial crushing in ordinary grooveless specimens A1 and A2 with that of externally grooved specimens S4 and S13 (see Figs 11 and 21) indicates obviously that application of the developed design method in the present study results in significant improvement of the crushing stability of metallic cylindrical tubes when subjected to axial loading. Even in case of the twisted concertina or mixed mode of deformation, the grooved shock absorber provides considerably

**Fig. 21** Views of different stages of axial crushing in specimen A1, derived from experimental tests

better crashworthiness characteristics and more stability during axial crushing in comparison with the grooveless specimen of A1 (see Figs 15 to 18 and 21). Moreover, in contrast with the previous design of grooved shock absorbers [**20**], which reduced the total absorbed energy compared with the grooveless specimen, the present design method does not affect this important crashworthiness parameter. In fact, in the present study, the objective to cut wide grooves from the outer surface of tubes is to divide their length to several portions and improve their crashworthiness characteristics. Moreover, the division of tube length with wide external grooves can decrease the maximum initial collapsing load of the tube, providing higher values of crush force efficiency. The introduction of wide external grooves affects the initial elastic resistance of the tube during axial compression.

## 9 CONCLUSIONS

In the present study, cutting circumferential wide grooves from the other surface of tubes with the aim of dividing their length into several portions is introduced as an efficient and reliable method to improve their crashworthiness characteristics. Numerical simulations of axial crushing in grooved specimens of various geometric parameters under axially quasi-static loading were performed. Also, an analytical model with consideration of strain hardening effects to predict the mean crush load of the shock absorber was proposed. Comparison between these results and experimental results, having been performed in this study, shows the high accuracy and reliability of theoretical studies. Through experimental, numerical, and analytical studies, major parameters in design are identified, and typical modes of deformation that may occur during axial compression of the shock absorber are characterized. Also, the load–displacement history and deformation mechanism of the shock absorber under both dynamic and quasi-static loading are described. Through both performed numerical and experimental studies, the energy absorption characteristics of the shock absorber under quasi-static loading are compared with that under impact loading.

It is shown that this design method can significantly control the shaping of axisymmetric folds while the shock absorber crushes axially, and can extend the limits of this most favourable collapsing mode of deformation. The effect of various geometric parameters of the shock absorber such as groove length and depth is studied both theoretically and experimentally. Results have shown that by adjusting these geometric parameters, various required mean crushing loads to protect different structures subjected to impact load from serious damages can be achieved. Also, by considering major geometric parameters in design, the shaping concertina mode of deformation can be guaranteed in axial collapsing of the shock absorber, resulting in a high safety factor. Moreover, unlike the conventional methods of energy absorption such as axial splitting and axial crushing of thin-walled structures, the proposed method has less sensitivity to the loading direction and condition. Favourably, it can be seen that cutting wide grooves along the tube length can decrease the elastic resistance of the structure against axial impact load, which leads to a considerable increase in crush force efficiency of the shock absorber.



## REFERENCES


1 **Johnson, W.** and **Ried, S. R.** Metallic energy dissipating systems. *Appl. Mech. Rev.*, 1978, **31**, 277–288.

2 **Alghamdi, A. A. A.** Collapsible impact energy absorbers: an overview. *Thin-Walled Struct.*, 2001, **39**, 189–213.

3 **Jones, N.** *Structural impact*, 1989 (Cambridge University Press, Cambridge).

4 **Reid, S. R.** and **Harrigan, J. J.** Transient effects in the quasi static and dynamic inversion and nosing of metal tubes. *Int. J. Mech. Sci.*, 1998, **40**, 263–280.

5 **Reddy, T. Y.** Tube inversion–an experiment in plasticity. *Int. J. Mech. Engng. Educ.*, 1989, **17**, 277–291.

6 **Al-Hassani, S. T. S., Johnson, W.,** and **Lowe, W. T.** Characteristics of inversion tube under axial loading. *Int. J. Mech. Sci.*, 1972, **14**, 370–381.

7 **Kinkead, A. N.** Analysis for inversion load and energy absorption of a circular tube. *Int. J. Strain Anal.*, 1983, **18**, 177–188.

8 **Stronge, W. J., Yu, T. X.,** and **Johnson, W.** Long stroke energy dissipation in splitting tubes. *Int. J. Mech. Sci.*, 1983, **25**(9–10), 637–646. Q6

9 **Reddy, T. Y.** and **Reid, S. R.** Axial splitting of circular metal tubes. *Int. J. Mech. Sci.*, 1986, **28**(2), 111–131. Q6

10 **Leu, A.** On the axial splitting and curling of circular metal tubes. *Int. J. Mech. Sci.*, 2002, **44**, 2369–2391.

11 **Andrews, K. R. F., England, G. L.,** and **Ghani, E.** Classification of axial collapse of circular tubes under quasi static load. *Int. J. Mech. Sci.*, 1999, **13**(1), 687–696.

12 **Bardi, F. C., Yun, H. D.,** and **Kyriakides, S.** On the axisymmetric progressive crushing of circular tubes under axial compression. *Int. J. Solids Struct.*, 2003, **40**, 3137–3155.

13 **Abramovicz, A.** and **Jones, N.** Dynamic axial crushing of circular tubes. *Int. J. Impact Engng.*, 1984, **2**(3), 263–281.

14 **Abramovicz, A.** and **Jones, N.** Transition from initial global bending to progressive buckling of tubes loaded statically and dynamically. *Int. J. Impact Engng.*, 1997, **19**(5/6), 415–437.

15 **Karagiozava, D.** and **Jones, N.** Inertia effects in axisymmetrically deformed cylindrical shells under axial impact. *Int. J. Impact Engng.*, 2000, **24**, 1083–1115.

16 **Karagiozava, D.** and **Jones, N.** Influence of stress waves on the dynamic progressive and dynamic plastic buckling of cylindrical shells. *Int. J. Solids Struct.*, 2001, **38**, 6723–6749.

17 **Guillow, S. R.** and **Lu, G.** Quasi-static axial compression of thin-walled circular aluminum tubes. *Int. J. Mech. Sci.*, 2001, **43**, 2103–2123.

18 **Hsu, S. S.** and **Jones, N.** Quasi-static and dynamic axial crushing of thin-walled circular stainless steel, mild steel and aluminum alloy tubes. *Int. J. Crashworthiness*, 2004, **9**, 195–217.

19 **Shakeri, M., Mirzaeifar, R.,** and **Salehghaffari, S.** New insights into the collapsing of cylindrical thin-walled tubes under axial impact load. *Proc. IMechE, Part C: J. Mechanical Engineering Science*, 2007, **221**, 1–17.

20 **Daneshi, G. H.** and **Hosseinipour, S. J.** Grooves effect on crashworthiness characteristics of thin-walled tubes under axial compression. *J. Mater. Des.*, 2003, **23**, 611–617.

21 **Abdul-Latif, A., Baleh, R.,** and **Aboura, Z.** Some improvements on the energy absorbed in axial plastic collapse of hollow cylinders. *Int. J. Solids Struct.*, 2006, **43**, 1543–1560.

22 **Singace, A. A.** and **El-Sobky, H.** Behavior of axially crushed corrugated tubes. *Int. J. Mech. Sci.*, 1997, **39**(3), 249–268.

23 **Reid, S. R.** and **Reddy, T. Y.** Static and dynamic crushing of tapered sheet metal tubes of rectangular cross-section. *Int. J. Mech. Sci.*, 1986, **28**(9), 623–637.

24 **Mamalis, A. G.** and **Johnson, W.** Quasi-static crumpling of thin walled circular cylinders and frusta under axial compression. *Int. J. Mech. Sci.*, 1983, **25**, 713–732.

25 **Shakeri, M., Salehghaffari, S.,** and **Mirzaeifar, R.** Expansion of circular tubes by rigid tubes as impact energy absorbers: experimental and theoretical investigation. *Int. J. Crashworthiness*, 2007, **12**, 493–501.

26 **Hanssen, A. G., Langseth, M.,** and **Hopperstad, O. S.** Static and dynamic crushing of circular aluminum extrusions with aluminum foam filler. *Int. J. Impact Engng.*, 2000, **24**, 475–507.

27 **Hanssen, A. G., Langseth, M.,** and **Hopperstad, O. S.** Static and dynamic crushing of square aluminium extrusions with aluminum foam filler. *Int. J. Impact Engng.*, 1999, **24**(4), 347–383.

Q6

28 **Santosa, S.** and **Wierzbicki, T.** Crash behavior of columns filled with aluminum honeycomb or foam. *Comput. Struct.*, 1998, **68**(4), 343–367.

29 **Alexander, J. M.** An approximate analysis of the collapse of thin cylindrical shells under axial loading. *Q. J. Mech. Appl. Math.*, 1960, **13**, 11–16.

30 **Hallquist, J. O.** LS-DYNA 3D: theoretical manual, Livermore Software Technology Corporation, Livermore, 1993.


## APPENDIX

### Notation

| | |
|---|---|
| $d$ | depth of grooves |
| $D_i$ | inside diameter of tube |
| $D_o$ | outside diameter of tube |
| $E_T$ | total absorbed energy of the shock absorber |
| $G$ | total weigh of the shock absorber |
| $H$ | total crushed length |
| $L$ | tube length |
| $M$ | weight of colliding mass |
| $M_o$ | plastic bending moment per unit length |
| $N$ | number of grooves |
| $P_m$ | mean crushing load |
| $P_{max}$ | maximum crushing load |
| $S_e$ | specific energy absorption factor |
| $t$ | tube wall thickness |
| $V$ | initial velocity of colliding mass |
| $W$ | length of thick portions |
| $W_D$ | required energy for creation of one fold |
| $W_T$ | work done by external work |
| $\lambda$ | length of wide grooves |
| $\rho$ | material density |
| $\sigma_o$ | flow stress |
| $\sigma_u$ | ultimate tensile stress |

JMES1709

**Queries**

S Salehghaffari, M Tajdari, and F Mokhtarnezhad

Q1 Please check and confirm all the language changes that have been to your manuscript.

Q2 Corresponding author email ID is mismatching between Cover sheet and Source file. We have followed as per source file.

Q3 Please check whether it should be “little” or “slight”.

Q4 Please check whether the added footnote for Table 3 is correct.

Q5 Please check the entity “getting the presented energy-absorbing device heavy” is not clear.

Q6 Please check the added page range in Refs 8, 9, and 27 is correct.